Spring 5-2020

The Functional Role of Glia in Peripheral Metabolic Tissue

Emma Paradie

THE FUNCTIONAL ROLE OF GLIA IN PERIPHERAL METABOLIC TISSUE

by

Emma Paradie

A Thesis Submitted in Partial Fulfillment
of the Requirements for a Degree with Honors
(Biology)

The Honors College

The University of Maine

May 2020

Advisory Committee:

Kristy Townsend, Associate Professor of Neurobiology, Advisor
Lynn Atkins, Instructor of Biology
Magdalena Blaszkiewicz, Postdoctoral Research Associate in the School of Biology and Ecology
Leonard Kass, Associate Professor of Biological Sciences
Sharon Tisher, Lecturer in the School of Economics and Preceptor in the Honors College

ABSTRACT

With the ever-growing pandemic of obesity comes a multitude of consequential morbidities, such as increased risk of heart disease and type II Diabetes Mellitus. Secondary to diabetes is diabetic neuropathy, the regression or dying back of nerves that often occurs in the extremities, leading to loss of sensation or pain. Additionally, aging is a risk factor for obesity, diabetes, and neuropathy. Responsible for the communication between the extremities and peripheral tissues, such as adipose (fat), and the brain, is the peripheral nervous system. The peripheral nervous system is the umbrella under which varying types of nerves are designated, including sympathetic, parasympathetic, and sensory nerves, which have been shown to innervate adipose tissue. Both the peripheral nervous system (PNS) and central nervous system (CNS) house glial cells, whose neuron-supporting functions are vital for maintaining homeostasis. Oligodendrocytes are the myelin-forming cells of the CNS, while Schwann cells are the myelin-forming cells of the PNS. Myelin is a fatty substance that ensheaths the axons of neurons, insulating them and allowing signals to be propagated through the body faster. Whereas crosstalk between glia and the immune system in the CNS is of increasing popularity in current research, much less is known about relative roles of glia and local immune cells in the PNS, particularly in adipose. This thesis delves into further investigating the types of glia that may be present in and interact with adipose tissue nerves. A better understanding of this interaction in adipose will be beneficial in uncovering mechanisms of proper energy balance and metabolic health, as well as potentially mitigating the progression of diabetic

neuropathy, or the death of peripheral nerves. To our knowledge, this thesis investigates the first ever immunopanning experiments for Schwann cells in adipose tissue.

ACKNOWLEDGEMENTS

I would like to thank Dr. Kristy Townsend for mentoring me and continuing to be my advisor through this project, despite her incredibly busy schedule. I would also like to thank Dr. Townsend and the rest of the Townsend Lab for really developing my love for science and excitement for research over the past three years. I have learned more academic, professional, and life lessons from being a part of this lab than I ever could have imagined.

I would like to thank Dr. Magda Blaszkiewicz for being my supervisor, training me in a variety of techniques in the lab, and teaching me how to do proper analysis for hours over zoom calls to practice "social distancing" during this COVID-19 pandemic.

I would like to thank Dr. Josh Havelin for assisting me through many of the experiments done for this thesis project.

I would like to thank the other members of my committee for answering many questions – be it one of academic merit, an abstract thought question, or one of general life advice – of mine throughout my years as an undergraduate student at UMaine.

Lastly, I would like to thank my friends and family for helping me keep my sanity throughout my entire undergraduate experience. It has been a time!

I'd like to thank the following resources for their financial support of this project:

- The University of Maine Center for Undergraduate Research
- The Charlie Slavin Grant
- Townsend Lab Grants and Funds

TABLE OF CONTENTS

LIST OF FIGURES AND TABLES

INTRODUCTION

Obesity Epidemic

The obesity epidemic is rapidly ever-growing around the world despite the increased recognition of the problem and its associated health risks. Adults having a body mass index (BMI) of 25.0 kg/m^2 to 29.9 kg/m^2 are defined as overweight, while those with a BMI of 30 kg/m^2 or higher are defined as obese[1]. According to the World Health Organization, worldwide obesity is nearly three times what it was in 1975, with a reported number of 650 million obese adults[2]. The issue at hand does not solely affect adults, however, and has had major implications in children as well. Children and adolescents from the ages of 2 to 18 are defined as overweight if they are in the 85^{th} to 94^{th} percentile of the population for their sex and age, and defined as obese if at or above the 95^{th} percentile[1]. Since the year 2000, the number of overweight children under the age of 5 in Africa has increased by roughly 50 percent, while in 2016, half of the world's overweight or obese population of children under the age of 5 lived in Asia[2]. Once a more drastic problem in high-income households, obesity has infiltrated into low- and middle-income households and countries as well.

Factors worldwide that have contributed in countries of all economic statuses include, but are not limited to, foods that are higher in sugar, fat, and salt, yet lack nutrients, inadequate amounts of sleep, chronic stress, eating while on-the-go, the increase in sedentary jobs as a result of technological advances and therefore decreased physical activity, and various levels of urbanization (i.e. more efficient transportation in

highly populated areas)[2,3]. In addition to the growing issue around the globe, the United States has also been greatly impacted by this epidemic. Prevalence estimates based on self-reported obesity published by the Centers for Disease Control and Prevention (CDC) showed that in 2011, all fifty states had an obesity prevalence of less than 35% and eleven states had a prevalence between 20%-25%. By 2018, however, self-reported obesity rates drastically increased, leaving nine states with an obesity prevalence of over 35% and only three states with a prevalence between 20%-25%[4]. In New England, Maine remains the state with the highest rate of obesity, which could be in correlation to both its aging and low-income populations.

Diabetes Mellitus

The human body composition largely depends on the balance between energy input versus energy expenditure. Factors that may be characterized as energy intake include diet, appetite, and digestion and nutrient absorption, while those characterized as energy expenditure may include basal metabolism, thermogenesis, and exercise/physical activity. As attributes on the energy intake side of the balance, such as diet, begin to outweigh energy expenditure, complications such as obesity begin to arise as a result. Individuals are subject to developing obesity based on varying factors, including sex, environment, genetics, age, and differences in the types of adipose tissue present[5,6].

Along with obesity comes the increased risk for comorbidities, some of which include stroke, hypertension, some cancers, and type 2 diabetes[1]. Of these, type 2 diabetes is one of the most common results of obesity. According to the American

Diabetes Association, “diabetes mellitus is a group of metabolic diseases characterized by hyperglycemia,” or increased blood sugar[7]. This sugar, or glucose, is a vital aspect in the body’s metabolic health. When there is a normal glycemic index, the body is healthy and able to carry out its functions. When there is an increased level of glucose in the blood for extended periods of time, however, metabolic complications can begin to arise.

Type 2 diabetes has historically been diagnosed mostly in adults, although the number of children and adolescents being diagnosed with type 2 diabetes over the past decade has increased drastically. Insulin is a hormone that is produced by the beta cells of the pancreas and is responsible for the uptake of glucose from circulating blood into the body’s cells. Therefore, glucose and insulin have an inverse relationship in a healthy individual, where a high level of glucose means there is currently a low level of insulin, and a high level of insulin would lead to lower levels of circulating glucose. Type 1 diabetes is the result of an autoimmune response in which the immune system mistakenly attacks the insulin-producing beta cells and thus the body is unable to make normal amounts of insulin[8]. This generally leads to such minute amounts of insulin in the body that individuals affected need to take insulin in order to survive. Type 2 diabetes is generally the result of prolonged, excessively high blood sugar levels. In this scenario, the beta cells of the pancreas try to make insulin to overcompensate for the high blood sugar levels. Eventually, the pancreas is unable to keep up with the amount of glucose and insulin resistance develops[8]. Nearly 85%-95% of all diabetic patients in high-income countries around the globe are diagnosed as type 2 diabetic patients, with the potential that the rate is even higher in low-income countries[9].

Diabetic Peripheral Neuropathy

Peripheral neuropathy is an unfortunately common consequence of patients diagnosed with diabetes. Peripheral neuropathy refers to physiological damage occurring in the peripheral nerve that is commonly presented in patients as distal degenerative polyneuropathy beginning in the extremities[10,11]. Roughly 20% of patients with type 2 diabetes will have diabetic peripheral neuropathy at initial diabetes diagnosis, and about 50% of all diabetic patients will inevitable develop diabetic peripheral neuropathy (DPN)[11,12]. DPN can have devastating effects on the lives of the patients effected and have a variety of implications. For instance, the regression of the nerve health can lead to loss of sensation and/or pain, which can in turn lead to much larger life-altering changes such as gait disturbance, fall-related injuries, and the development of ulcers on the feet, frequently a preempting lower limb amputation[11].

There are various categories of DPN, with the most common being distal symmetric polyneuropathy. This type of DPN constitutes nearly 75% of all diabetic neuropathies and can be characterized in one of three ways; primarily small-fiber, primarily large-fiber, or a combination of the two[12]. The remaining approximate 25% of diabetic neuropathies include categories such as treatment-induced neuropathies, mononeuropathies, and autonomic neuropathies – the most similar to distal symmetric polyneuropathy despite being mostly non-sensory[12]. There are currently no treatments for neuropathy, only medications prescribed in hopes of making patients more comfortable, weight management, blood glucose control, and physical therapy[11,12].

A lot of aspects contribute to the peripheral nerve not maintaining its proper function. The cell body is housed just outside of the spinal cord in what is called the

dorsal root ganglion (DRG) or anterior horn cell, and this is where damage can often begin. The damage can then progress through the rest of the cell and axonal projection, including the myelin sheath wrapped around it[11]. In patients with diabetes, the endoneurial microvessels are damaged and therefore cause structural abnormalities in diabetic nerves[13]. A decrease in the thickness of the basement membrane of these endoneurial microvessels has also shown to be correlated to decreased myelinated fiber density[13]. Excessive glycation is common in diabetic nerves, and advanced glycation end-products (AGE) deposition in various structures of peripheral nerve tissues, including the axoplasms of Schwann cells, presents an inverse correlation with myelinated nerve fiber density. In fact, diabetic mice without the gene for the receptor for AGE (RAGE), have shown protection against neuropathy[13]. Sustained hyperglycemia leads to oxidative stress and thus the generation of free radicals, eventually causing mitochondrial damage and leading to downstream effects of reduced neurotrophin-3 (NT-3) and nerve growth factor (NGF)[13]. Large-fiber DPN causes patients to be particularly susceptible to developing foot ulcerations as a result of the loss of sensation in the foot as well as gait disturbance. Common symptoms often described by the population of patients with this type of neuropathy are numbness, tingling, and discomfort[11]. This is a consequence of the "large-diameter myelinated A-beta somatic fibers" being affected by (generally longstanding) neuropathy, because these fibers are notorious for their role in touch sensation and joint position[11]. In comparison, small-fiber DPN affects mainly "small diameter thinly myelinated A-delta fibers" and "unmyelinated C somatic fibers" responsible for transmission of cold/mechanical pain information, and thermal, mechanical, and chemical pain signals respectively[11]. As a result, patients often

complain of painful sensations such as burning and stinging and present with minimal ability to sense external painful and thermal stimuli in conjunction with decreased proprioceptive sensation[11].

Nerve Innervation and Neuropathy in Adipose Tissue

In order to maintain a healthy metabolic balance, the exchange of information between the brain, particularly the hypothalamus, and peripheral tissues is critical. Communication to the brain from the periphery is not only signals sent from circulating nutrients and endocrine factors, but also consists of signals from afferent sensory nerves and efferent sympathetic nerves relaying information to and from the periphery[14].

There are two major divisions of adipose, or fat; brown adipose tissue (BAT) and white adipose tissue (WAT). While WAT is notorious for its role as the major site of energy storage, BAT is predominantly known for its thermogenic and energy expenditure function[5]. It is known that BAT is in relatively high abundance in newborns, but prevalent in lower amounts of adult humans. Recent research has revealed, however, that brown adipogenesis can be induced in white fat through various physiological stimuli, including cold exposure and sympathetic activation[15]. Additionally, adipose tissue is responsible for secreting various circulating endocrine factors that contribute to the activation of lipolysis in WAT or thermogenesis in BAT[19]. An example of this is the release of norepinephrine by sympathetic nerve terminals as a positive regulator of lipolysis. For these reasons, it is typical for an excess of WAT to be associated with the obesity epidemic and fat accumulation, while BAT or the browning of white adipose tissue could contribute to the protection against obesity. One of the major defining

characteristics of obesity is an increase in fat cell number, making it important to understand the processes under which this may occur, or how it may be affecting other physiological processes[16]. Browning and adipocyte mass homeostasis are largely dependent on nerve supply to the WAT. The sympathetic nervous system (SNS) is known for conveying energy expenditure signals from the CNS to peripheral tissues[17]. Surgical denervation of SNS fibers in WAT has been shown to increase the number of adipose cells and thus increase fat pad mass, although there was no increase in the size of the fat cells themselves[16,18]. SNS innervation of WAT is known for its role in modulating fat cell proliferation through the release of norepinephrine (NE) that acts to inhibit fat cells from proliferating freely[18]. This result differs from that of strictly sensory denervation that shows an increase in the size of fat cells, but no change in overall fat pad mass[18]. This notable difference is important for investigating the different roles of both sensory and sympathetic innervation in white adipose tissue, and their contribution to maintaining proper energy balance.

Historically, peripheral neuropathy has been noted as a metabolic disease in tissues such as that of the skin and distal extremities, but it has more recently been shown to have other implications and occur in various other organs, including adipose. While there is a continued need for further study in metabolic functions and mechanisms, it has been shown in a cohort of experiments including aging, obesity, and diabetes, that WAT from both mice and humans fails to maintain healthy innervation[17]. Failure to maintain proper innervation can have serious implications in the energy balance roles of the nerve fibers affected, as we know these nerves are responsible for processes such as lipolysis (releasing fatty acids through the breakdown of fats) and thermogenesis (the generation

of heat, particularly in BAT due to UCP-1)[17]. Leptin, a hormone produced by adipose tissue, is responsible for the breakdown of white adipose tissue via its communication with the brain. This lipolytic effect is knowingly modulated by sympathetic nerve fibers[20]. Thus, denervation of sympathetic nerves in adipose tissue can also have detrimental effects to the tissue's health.

Such findings further the necessity for looking into possible solutions and treatments for neuropathy, particularly that of adipose tissue. Using an axonal growth cone marker (GAP43), a pan-neuronal marker (PGP9.5), and a sympathetic nerve marker (tyrosine hydroxylase or TH), it has been depicted that cold exposure intervention enhances nerve plasticity in the peripheral adipose tissue[17]. Cold exposure interventions in visceral adipose tissue (VAT) have also been shown to induce significant weight loss in mice fed high-fat diets (HFD), as well as significant increase of metabolic responses, and the remodeling of the adipose[21]. This remodeling in subcutaneous WAT involves the increase in sympathetic fiber innervation shown through expression of tyrosine hydroxylase (TH), a common dopaminergic marker, as well as pan-neuronal marker TUBB3. Other factors that contributed to the adipose remodeling were angiogenesis, browning of the adipose tissue, and an induced accumulation of extracellular matrix around the VAT adipocytes[21].

Risk of Neuropathy Increases with Age

According to the U.S. Census Bureau, Vintage 2018 Population Estimates, Maine has the highest population percentage of individuals sixty-five or older in the nation[22]. Aging individuals are at higher risk for the development of type 2 diabetes and therefore the development of neuropathy. The level of risk and severity for the development of diabetic neuropathy in an aged population is dependent upon a plethora of factors, including hyperglycemia, hypertension, and smoking[23]. PGP9.5, a pan-neuronal marker, exemplifies a significant decrease in inguinal subcutaneous WAT of both mice and humans is seen as age increases, indicating the severe loss of nerve innervation in this tissue[17]. Additionally, increased age in mice correlated with a trend for increased subcutaneous WAT weight and a trend for decreased levels of the SNS marker, TH[17]. Aged populations with diabetic neuropathy are also at a high risk of exhibiting microvascular complications, as well as decreased innervation surrounding the vasculature in their subcutaneous WAT depots[17,23]. Loss of proper vascular function could be a crucial factor, as it signifies loss of well-distributed nutrients to the affected regions.

The Importance of Glia in Nerve Health

Glia are a crucial component of the neurological system as they are characteristically known as the neuronal support cells. The word “glia” is derived from the Greek word for “glue,” which is fitting given the function of these cells[24]. There are various types of glia throughout the body, with unique types in varying niches. For instance, glia such as astrocytes, microglia, and oligodendrocytes reside in the CNS, Schwann cells and satellite glia are characteristic of the PNS, and the enteric nervous

system has to date identified a handful of residential glia types in the gut. There are a few characteristics that strongly distinguish glia from their neuronal counterparts. To begin with, nerve cells interact with one another and communicate via electrical signaling (often referred to as action potentials) and interactions at the synapse, while glia cells simply contribute supportive functions in these processes, such as modulating neurotransmitter release and uptake and the rate at which signals are propagated along the nerve cell[24].

While properties such as these are known to be functions of glia, there are still so many more functions that have yet to be discovered. In addition to the variety of these cells, their locations and interactions with other cell types make it difficult to pinpoint such functions. The most research and attention has thus far been directed towards glia in the central nervous system, particularly the brain. In the brain and spinal cord, one of the most studied glial cell types is astrocytes. These cells have a very distinct morphological structure, leading them to frequently be characterized as star-shaped. Throughout the brain, there is an exuberant number of classifications of astrocytes based on morphology and location, creating much difficulty in determining the various roles and implications of each[25]. Some of the roles of astrocytes consist of regulating blood-brain barrier permeability, which is consequential in preventing the entrance of harmful substances into the brain, including toxins and bacteria that could cause damage to the brain tissue[25]. It has been shown that astrocytes express the same genes as other cell progenitors, giving them the ability to be proliferative. This function can have implications if proliferation gets out of hand, leading to inflammation of the astrocytes which is generally characterized by an upregulation of glial fibrillary acidic protein

(GFAP). This inflammation state can sometimes lead to the loss of proper astrocytic function, leading to cellular senescence and showing correlations to many neurodegenerative diseases, including Alzheimer's disease, Huntington's disease, and recently exhibiting roles in amyotrophic lateral sclerosis (ALS)[25].

Another glial cell type of high importance in the brain and spinal cord is microglia. Microglia are notorious for being the "resident macrophages" of the CNS, meaning they are crucial to phagocytosis in this region of the body[26]. Phagocytosis is a process required for healthy pruning of the brain and includes recognizing, engulfing, and digesting foreign, harmful, or unnecessary particles or debris[26]. Not only is this function important for the regulation of both innate and adaptive immune responses, but it is continuing to prove necessary for modulating pathological processes[27]. The need for further research regarding the role of microglia in maintaining a healthy brain versus contributing to brain damage remains necessary. Techniques such as using mutant rodents or microglial depletion assays are beginning to open up the possibility of such a research and have begun showing results indicating that the loss of microglia leads to cognitive developmental deficits in rodents[27]. There is even speculation of the role of microglia in modulating adult neurogenesis[27].

The last of the significant glia trio in the CNS is oligodendrocytes. Oligodendrocytes originate from oligodendrocyte precursor cells and are infamous for their role in myelination[28]. Oligodendrocytes are able to wrap their branches around multiple neuronal axons, which can be an extremely metabolically taxing process, leaving these cells susceptible to cytotoxic or excitotoxic infiltration[28]. Affected oligodendrocytes can therefore have function alterations that can lead to demyelinating

diseases like multiple sclerosis or other pathological diseases like schizophrenia and Alzheimer's disease[28].

While there are three distinguishable categories of glia in the CNS, there are only two that are recognized in the PNS – satellite glia cells that reside the ganglia and Schwann cells in the peripheral nerves. In rodent models, satellite glia have been shown to control cholinergic transmission in sympathetic neuron-to-neuron interactions[29]. Satellite glia have also been shown to contribute to overall sympathetic neuronal health and survival, in addition to promoting synapse formation[29]. Despite this knowledge, there is still much research to be done to further understanding all of the functions of satellite glia. Schwann cells, who are often discussed in regards of myelinating peripheral nerves, are present in the body in many different developmental stages, correlating them to a variety of different roles – many of which still require further research. Lack of knowledge about the role of Schwann cells in adipose tissue, their role in nurturing neurons, and their communication processes with other cells – particularly immune cells – leaves the field with exciting potential for discovery.

Schwann Cell Development

Schwann cells are somewhat of an enigma in the peripheral nervous system. Although they are notorious for their role in axonal myelination, more and more research regarding Schwann cells continues to reveal interesting additions to the responsibilities of these cells. The lack of knowledge regarding the wide array of Schwann cell functions and communications is invigorating, allowing for the development of innovative avenues to study hypotheses of their functions. Extrapolating the relatively little amount of

information we know about glia in the CNS and hypothesizing how similar roles may be carried out in the PNS by Schwann cells could lead to endless new discoveries about the importance of this cell group.

During embryonic development, the neural crest gives rise to neural crest stem cells, which are in turn responsible for giving rise to a multitude of differing sub-lineages, including that of Schwann cells[30]. Schwann cell lineage includes many different variations of these specialized cells, as can be seen in Figure 1.

Schwann Cell Precursors (SCP) are the first developmental stage in Schwann cell lineage when beginning to differentiate from neural crest cells. These cells maintain some stem-cell-like characteristics after this initial differentiation, allowing them to be multipotent, a feature shared amongst early glial cells in both the PNS and CNS[30]. As multipotent cells, SCPs also have the ability to differentiate into cells such as melanocytes, endoneurial fibroblasts, parasympathetic neurons, chromaffin cells, and tooth pulp cells[30]. Additionally, experiments have shown that parasympathetic nerves are also capable of being derived from SCPs, giving SCPs a list of differentiation possibilities[31,32]. *Myelin protein zero (mpz)* is a gene that encodes for myelin protein zero, notorious for its expression in myelinating Schwann cells. Research has shown, however, that *mpz* is also expressed at low basal levels in Schwann cell lineage long before they are differentiated into myelinating Schwann cells, as it has been detected in SCPs, immature Schwann cells, and even a small population of neural crest cells before axonal outgrowth from the spinal cord has even begun[30]. SCPs are most often associated with large nerve branches, in which they embed themselves amongst bundles of axons as well as among the axons at the nerve surface. After the conversion of neural

crest cells to SCPs in nerves, there is a gene expression change that occurs in hundreds of genes – generally an upregulation of functional classes, such as molecules involved in cell differentiation and transcription factors[30]. These factors are important, because they are often the genes encoding for many of the proteins used to identify Schwann cells, such as myelin basic protein (MBP) and desert hedgehog (Dhh), and S100b [30,33].

Next in the Schwann cell lineage are immature Schwann cells. This developmental stage occurs during embryonic days 15-16 in mice and shows association between these cells, connective tissue, basal lamina inside nerves[30]. Part of the Schwann cell membrane is the basil lamina, which surrounds the cell and is responsible for housing extracellular matrix molecules, such as laminin[34,35]. In conjugation with the laminin receptor, β1-integrin, and other signaling cascades downstream, various laminin isoforms work to configure the appropriate alignment of Schwann cells to axons[36]. Components of the extracellular matrix regulate function, architecture, and function of myelin during the development of Schwann cells[35]. Laminin and its role differ throughout Schwann cell lineage, depicting a vital role in stimulation of radial sorting. Radial sorting is a process through which immature Schwann cells – originally congregated around groups of axons – continue to proliferate so that there is a 1:1 ratio of Schwann cells to axons[24,26,27]. Once at this 1:1 ratio, the cells in rodents typically become “pro-myelin” cells and go on to form myelinating Schwann cells, but in humans, there are a significant number of axons that remain unmyelinated at the 1:1 ratio, eventually going on to form Remak bundles, or non-myelin Schwann cells[30].

Schwann cell plasma membranes are constituted of a high lipid content and cholesterol, playing an important role in the process of myelination[34]. Schwann cells

ensheath axons in a methodical manner; the nucleus remains fixed, but the inner turn of the Schwann cell membrane creates the myelin sheath by spiraling around the axon to continuously build membranous layers, known as lamellae[34]. The amount of Neuregulin I-type III exposed on the membrane of the axon sends signals to the Schwann cell whether or not it should myelinate, as well as dictating how much myelin should be produced by myelinating Schwann cells[33,37]. Proliferation of Schwann cells occurs before cells have gone through radial sorting, as myelinating Schwann cells generally do not undergo division. Increased proliferation generally coincides with precursor to immature Schwann cell conversion and appears to be correlated to an increase of intracellular cAMP[33]. Myelin is unique in its composition of mostly lipids with some low-molecular weight proteins, contributing to how densely packed it is[36]. The mere structure of myelin indicates that there is likely an unusual form of transport within the cell. One of the difficulties in studying this topic in cell biology, is that the myelin is packed so tightly that it is difficult to view with light microscopy. Although not the same as Schwann cells, oligodendrocytes, the myelinating cells of the CNS, have very similar composition to that of Schwann cells, and have been able to be cultured and studied to an extent *in vivo*[36]. Results of culturing oligodendrocytes indicate that vesicle transport is confined to the cell body of the cell and doesn't carry through the layers of myelin sheath. Myelin is known to be composed of the cytoplasmic protein myelin basic protein (MBP) and proteolipid protein (PLP), the latter of which is an integral protein and may be an influential factor in membrane trafficking[38].

Mitochondria and other cytosolic components are located in the outermost layer of myelinating Schwann cells. This is termed the abaxonal region and is separated from

the region of the cell that is directly attaching to the axon by myelin sheath. Experiments indicate that ATP is released from nerve axons, signals to the abaxonal membrane of myelinating Schwann cells, and is therefore able to communicate with the mitochondria housed there[39]. In fact, extracellular ATP increases with increasing axonal firing and leads to activation of purinergic receptors. This is important, as purinergic signaling is shown to enhance Schwann cell mitochondrial Ca^{2+} release, and this increased intracellular Ca^{2+} concentration in the mitochondrial matrix enhances ATP production[39]. In Schwann cells during catabolic processes, lactate (that has been converted from glycogen) is taken by monocarboxylate transporters, oxidized to pyruvate, and then the newly created pyruvate is brought to the axon to join the Krebs cycle and produce ATP, just as typical eukaryotic cell metabolism[40]. As research continues in this field, indicating the importance of Schwann cell mitochondria in myelination and nerve health, there are hypotheses that Schwann cell mitochondrial dysfunction could contribute to neuropathic peripheral nerves[41].

Unlike the myelinating cells of the CNS, oligodendrocytes, Schwann cells are not fixed once in these states, allowing them a characteristic deemed as plasticity, through which these cells are able to convert themselves into regenerative or repair cells in a time of injury[42]. These repair cells, deemed “Bungner” cells, are converted to such cells from myelinating Schwann cells via the transcription factor c-Jun and reenter the cell cycle after injury to help with reparations to injured nerves[43]. The mechanistic conversion back into myelinating cells still requires further research, as does the assumed role of non-myelinating Schwann cells to also be converted into repair Schwann cells. There is continuing research, however, that indicates the role of repair Schwann cells in

supporting damaged neurons while promoting axonal regrowth and assisting those axons in finding their targets, recruitment of macrophages, and clearing unnecessary myelin[44]. Additionally, it is known that Schwann cells are capable of a type of autophagy deemed "myelinophagy," but recent research has also focused on the concept of "demyelinating" Schwann cells and their roles in demyelinating neuropathies[45]. These cells are believed to play an important role in myelin clearance in conditions both with and without intact axons, seeming to play quite similar roles to the repair Schwann cell described by Jessen and Mirsky – both with potentially vital roles in peripheral neuropathies[45].

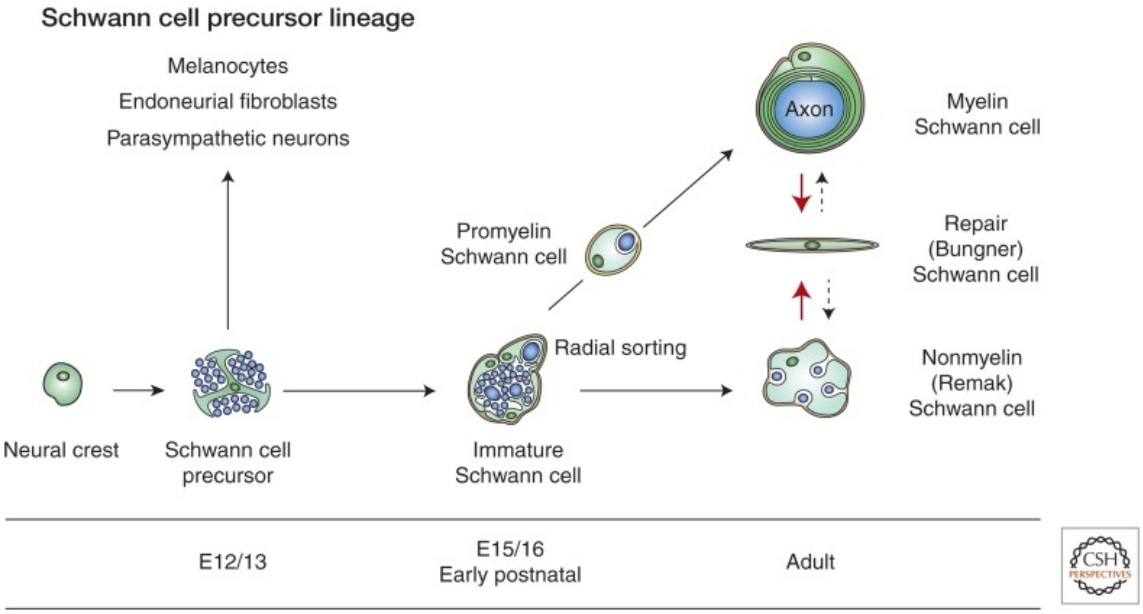

Figure 1. Schwann cell lineage: from neural crest cell to myelinating and non-myelinating Schwann cells (Taken from Jessen et. al., 2015; *Schwann cells: development and role in nerve repair)*.

Immunopanning

With limited ways of isolating cells and their respective functions, the first instance of any sort of "panning" was in the year 1980, and the experiment's goal was to isolate and culture astrocytes from the brain by negatively selecting unwanted immune cells[46]. Ben Barres took full advantage of the upcoming technique. He began using it in 1988 to isolate and purify various cell types from retinal ganglion cells, after which point he continued to use it for an extensive number of experiments and published papers[47]. This was a successful technique for Barres as it was relatively cheap and quick, while providing reliable results. Immunopanning has been a procedure used predominantly in the field of neuroscience surrounding the CNS, but has made a few appearances in experiments for the PNS. One of the earliest documented isolations of Schwann cells through a similar, simple "panning" method was done by Assouline and colleagues in 1983 with a peripheral nerve taken from a rat model[48].

In the experiments conducted for this thesis, the written protocol was adapted from one published by Cold Spring Harbor[49]. The protocol from Cold Spring Harbor was for isolating Schwann cells from the sciatic nerve – the only peripheral tissue (of any kind) to have used immunopanning. Given that the sciatic nerve and adipose tissue are quite different in mass, fibrosity, and other constituents, it was necessary for there to be a learning curve for adaptations to be made to the protocol. The most eminent part of the protocol needing refining was the division for the digestion of the adipose tissue.

Fluorescence-activated Cell Sorting (FACS)

One of the most commonly used techniques in separating cell sub-populations within a given population is through using fluorescent labeling. Tissues are digested with protocols specific to that given tissue and cells are isolated following a protocol. Once the cells are isolated, they are labeled with fluorophore-conjugated antibodies that correlate to the specific proteins of interest. During sorting, each population of cells (for instance, that of adipose taken from one animal) is placed into a flow cytometer. One at a time, the cells go to leave the nozzle tip of the machine. As they do so, they enter a single droplet that is passed through a laser to detects its fluorescent label and is then given an electric charge based on the labeled fluorescence of the cell. In combination with the given charges, deflection plates cause cells to either be attracted to or repelled from them and into their relative collection tubes [50].

FACS is a very successful and well-practiced method for sorting cells based on their phenotypes, but does require the proper, expensive equipment and someone who is well versed in using the equipment. Although FACS certainly has its limitations, it is also more beneficial in comparison to other techniques, such as magnetic-activated cell sorting (MACS), in that the flow cytometry allows more flexibility and accuracy in distinguishing the phenotypes of various cells[51].

MATERIALS AND METHODS

I. Experimental Model and Animal Subject Details

For all immunopanning and FACS experiments, C57BL/6J male and female mice (Jackson Laboratory, Bar Harbor, ME; *Jax 000664*) were used with IACUC approval and regulations, as seen in Appendix A.

II. Immunopanning

Petri dishes were coated with 30 µL of secondary antibody (dish 1: goat anti-rat IgG, dish 2: goat anti-mouse IgG + IgM, dish 3: goat anti-mouse IgM, µ chain specific) in 10 mL of 50mM Tris-HCl. Plates were gently shifted from side to side to allow for the bottom surface of each plate to be completely covered with solution and then incubated in 4ºC overnight. The next morning, the dishes were rinsed three times with D-PBS and a solution of 0.2% BSA in D-PBS was added to each dish and left to incubate at room temperature. After 30 minutes, the BSA solution was aspirated and each plate was coated with their respective primary antibodies (dish 1: CD45, dish 2: Thy1.2, dish 3: O4). The plates were left to incubate at room temperature for a minimum of 2 hours. While plates were incubating, mice were euthanized by CO_2 asphyxiation with secondary cervical dislocation. Inguinal scWAT depots were dissected, weighed, and minced in a Petri dish containing a collagenase/DMEM (high-glucose, serum-free) solution (concentration of 2mg/mL). The minced adipose depot was then transferred to a 50 mL conical tube with 10 mL collagenase/DMEM solution. DRG and sciatic were also dissected and collectively pooled into two 15 mL tubes with 3.5 mL collagenase/DMEM solution. The

covers of the conical tubes were loosely capped to prevent cell death. The samples were placed in a shaking water bath at 37ºC and triturated every 15 minutes with glass pipettes of various bores until adipocytes were floating and there were no chunks of tissue remaining. Adipose solutions were then filtered into new tubes through 100 µm filters, followed by a filter wash of 2 mL low-ovo working solution. Samples were then centrifuged at 500g for 10 minutes to pellet the tissue. The collagenase/DMEM cocktail was then aspirated out of each tube and replaced with 10 mL of low-ovo working solution. Cells were then resuspended in 5 mL of panning buffer, filtered through 100 µm cell strainers 1 mL at a time to remove any large pieces of debris, and the filters were each washed with an additional 5 mL of panning buffer. Cells were left in 37ºC for 30-45 minutes to allow for cell recovery. Next, the primary antibodies were aspirated from the Petri dishes and the dishes were each washed three times with D-PBS. Samples were poured first onto their corresponding CD45 plates and incubated at room temperature for 20 minutes (lightly shaken at 10 minutes). Non-adherent cells were then transferred from their CD45 plate to their Thy1.2 plate and incubated at room temperature for 20 minutes (lightly shaken at 10 minutes). Cells that had adhered to the CD45 plate were lifted from the plate using 200 µL of 2.5% trypsin in 4 mL of equilibrated EBSS and frozen in 50 µL of Trizol Reagent, manually disrupted via trituration, and stored at -80ºC. Non-adherent cells were then transferred from their Thy1.2 plate to their O4 plate and incubated at room temperature for 20 minutes (lightly shaken at 10 minutes). Cells that had adhered to the Thy1.2 plate were lifted from the plate using 200 µL of 2.5% trypsin in 4 mL of equilibrated EBSS and frozen in 50 µL of Trizol Reagent, manually disrupted via trituration, and stored at -80ºC. Non-adherent cells on the O4 plate were then frozen in 50

µL of Trizol Reagent, manually disrupted via trituration, while cells that had adhered to the O4 plate were lifted from the plate using 200 µL of 2.5% trypsin in 4 mL of equilibrated EBSS and frozen in 50 µL of Trizol Reagent, manually disrupted via trituration, and both populations were also stored at -80ºC.

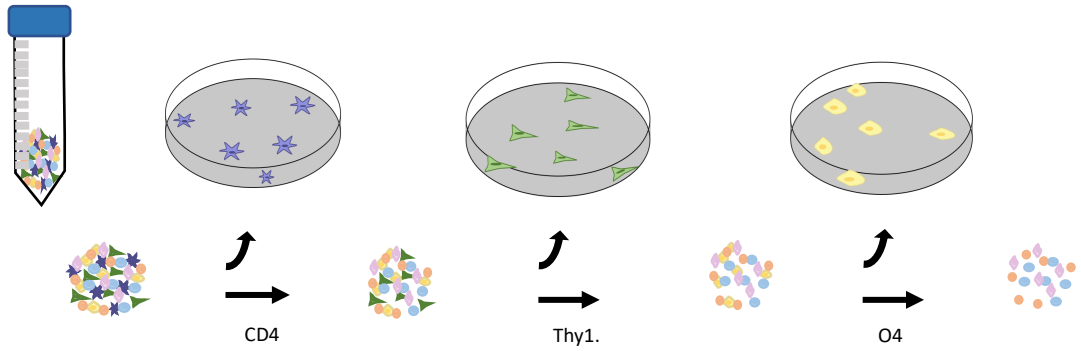

Figure 2. Schematic of the immunopanning procedure used for these experiments

III. Fluorescence-Activated Cell Sorting (FACS) Analysis

Mice were euthanized by CO_2 asphyxiation with secondary cervical dislocation. Inguinal scWAT depots were dissected, weighed, and minced in a Petri dish containing a collagenase/DMEM (high-glucose, serum-free) solution (concentration of 2mg/mL). The minced adipose depot was then transferred to a 50 mL conical tube with 10 mL collagenase/DMEM solution. DRG and sciatic were also dissected and collectively pooled into two 15 mL tubes with 3.5 mL collagenase/DMEM solution. The covers of the conical tubes were loosely capped to prevent cell death. The samples were placed in a shaking water bath at 37ºC and triturated every 15 minutes with glass pipettes of various

bores until adipocytes were floating and there were no chunks of tissue remaining. Samples were then filtered through 100 μm cell strainers into 50 mL tubes and rinsed several times with DMEM. The samples were then centrifuged at 500g for 10 minutes to separate the adipocytes and SVF. The SVF was collected by aspirating out the solution, incubating the pellet in 500 μL of red blood cell (RBC) lysis buffer for 2 minutes on ice. Following RBC lysis, 2 mL of DMEM (with serum) was added to stop the lysis and the samples were centrifuged at 500g for 5 minutes at 4ºC. DMEM was decanted and cells were resuspended in 100 μL FACS buffer (PBS with 5% FCS). Next, 4 μL of FACS block per sample and sat on ice for 15-20 minutes. 500 μL of FACS buffer was added and samples were spun at 1800 rpm for 5 minutes. Samples were then resuspended in 100 μL of FACS buffer with FACS antibodies (CD45-AF700, P75-VIOBRIGHT FITC, O4-APC) for 20 minutes. Cells were then washed 2 times by centrifugation at 1500 rpm for 5 minutes and resuspended in 300 μL of ice cold FACS buffer. The cells were kept in the dark and on ice for the transport to The Jackson Laboratory until the scheduled time of analysis. During analysis, cell populations were sorted into Trizol Reagent in Eppendorf tubes.

IV. RNA Extraction

For RNA extraction, 2 small scoops of bullet blender beads was added to each population of cells in their Safe-lock Eppendorf tubes, which were then paced into the Bullet Blender on setting 6 for 3 minutes. Samples were centrifuged at 12,000g for 15 minutes in a refrigerated centrifuge. The supernatant was pipetted off (avoiding the tissue debris and beads) into a new 1.5 mL nuclease-free tube. The tubes sit for 5 minutes at room temperature. One volume of ice-cold 95-100% EtOH to each sample and mixed by vortexing. Sample was immediately loaded into a labeled column tube and spun at 12,000g for 30 seconds. The flow-through was discarded into a waste beaker and the remainder of the sample was re-run in the same manner until all RNA was bound to the column. After the last spin, the column was transferred to a new collection tube and 400 µL of RNA Pre-Wash buffer was added to the column and spun at 12,000g for 30 seconds with flow through discarded. This step was then repeated. 700 µL of RNA Wash Buffer was added to the column and then spun at 12,000g for 1 minute. Flow-through was discarded and the empty column was spun at 12,000g for 2 minutes with the cap open to dry the column. The column was transferred to a new 1.5 mL nuclease-free tube and 50 µL of nuclease-free water was added directly to the middle of the column. This sat for 1-5 minutes on ice to absorb the RNA from the column and spun at 12,000g for 1 minute to elute RNA. Samples stored at -80ºC.

V. Qubit Analysis

For high sensitivity RNA measurement with Qubit analysis, Qubit Working Solution for all tubes (standards, spike-in, and sample tubes) was prepared by diluting the RNA Reagent (200x) into RNA HS Buffer, such that there were 180 µL per sample tube. 180 µL of Working Solution was pipetted out into two Standard tubes, followed by 10 µL of nuclease-free water to each tube and 10 µL of Standard #1 and Standard #2, to their respective tubes. Next, Master Mix was prepared by adding Standard #2 (10ng/µL) as our spike-in RNA, and nuclease-free water to the tube containing the remaining Qubit Working Solution. 199 µL of the Master Mix was aliquoted into each sample tube and spike-in control, followed by 1 µL of each RNA sample to its respective sample tube, and then 1 µL of nuclease-free water to each respective spike-in control tube. The solution was vortexed for a few seconds and then spun down in the centrifuge for a few seconds. Tubes were allowed to incubate at room temperature for two minutes in the dark to allow the Qubit assay to reach optimal fluorescence. Standardization was first performed in the Qubit by first inserting the Standard #1 tube, hitting measure, and then inserting the Standard #2 tube and hitting measure. Next, the sample tubes were inserted and measured in a recorded order. Values for final RNA levels were determined by putting the data onto a flash drive and entering the numbers into an Excel file, where the RNA Spike-in control values were able to be subtracted from the final read RNA values, therefore determining the final RNA values in each sample.

VI. Statistical Analysis

For statistical analysis, statistical calculations were conducted in either Excel or GraphPad Prism software (La Jolla, CA, USA), using Student's t-test and one-way and two-way ANOVAs. All plots represent mean +/- SEM. For all figures, *p < 0.05, **p <0.01, ***p < 0.001, ****p < 0.0001.

RESULTS

I. Immunopanning Trial I for O4 Positive Cells in subcutaneous white adipose tissue

At 15 weeks old, four male C57BL/6JUM mice showed no significant difference in RNA levels across the cell populations deemed CD45 positive, Thy1.2 positive, O4 positive, and O4 negative (Fig. 3). RNA levels in all populations were extremely low and therefore had to be quantified using Qubit technology rather than Nanodrop. RNA levels in the CD45+ population ranged from 0.66 ng/μL – 1.56 ng/μL. RNA levels in the Thy1.2+ population ranged from 0.71 ng/μL – 0.97 ng/μL. RNA levels in the O4+ population were between 0.44 ng/μL – 1.05 ng/μL. RNA levels in the O4- population were between 0.76 ng/μL – 1.24 ng/μL. While there was no statistical significance, it can be seen from these numbers that the O4+ population had the smallest number for the low end of the range.

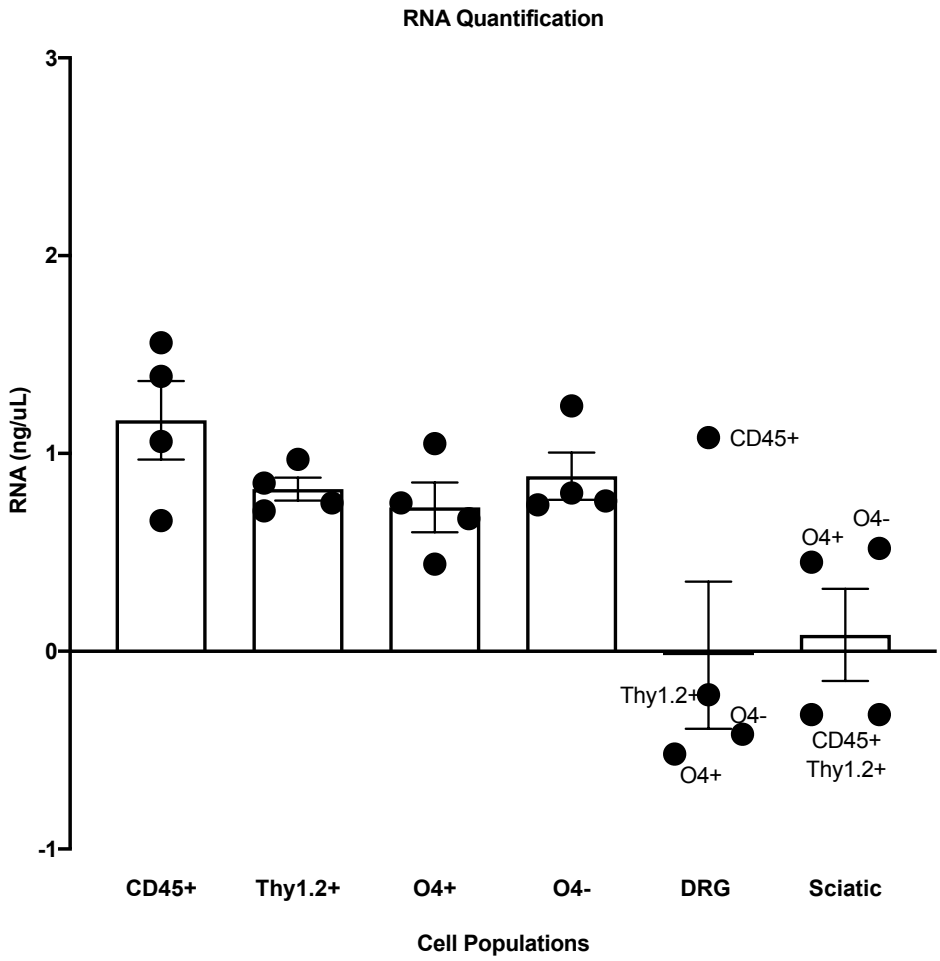

Figure 3. RNA quantification of different cell populations in Immunopanning Trial 1

II. Immunopanning Trial II for O4 Positive Cells in subcutaneous white adipose tissue

At the ages between 13 to 18 weeks, five male C57BL/6JUM mice showed a significant difference in RNA levels between the CD45 positive Thy1.2 positive populations (Fig. 4). RNA levels were again extremely low across the board, requiring analysis by Qubit technology rather than Nanodrop. RNA levels in the CD45+ population ranged from 0.65 ng/µL – 3.36 ng/µL. RNA levels in the Thy1.2+ population ranged from -0.6 ng/µL (indicating extremely low levels or an error in extraction?) – 0.64 ng/µL.

RNA levels in the O4+ population ranged from 0.06 ng/µL – 0.39 ng/µL. RNA levels in the O4- population range from 2.51 ng/µL – 8.52 ng/µL.

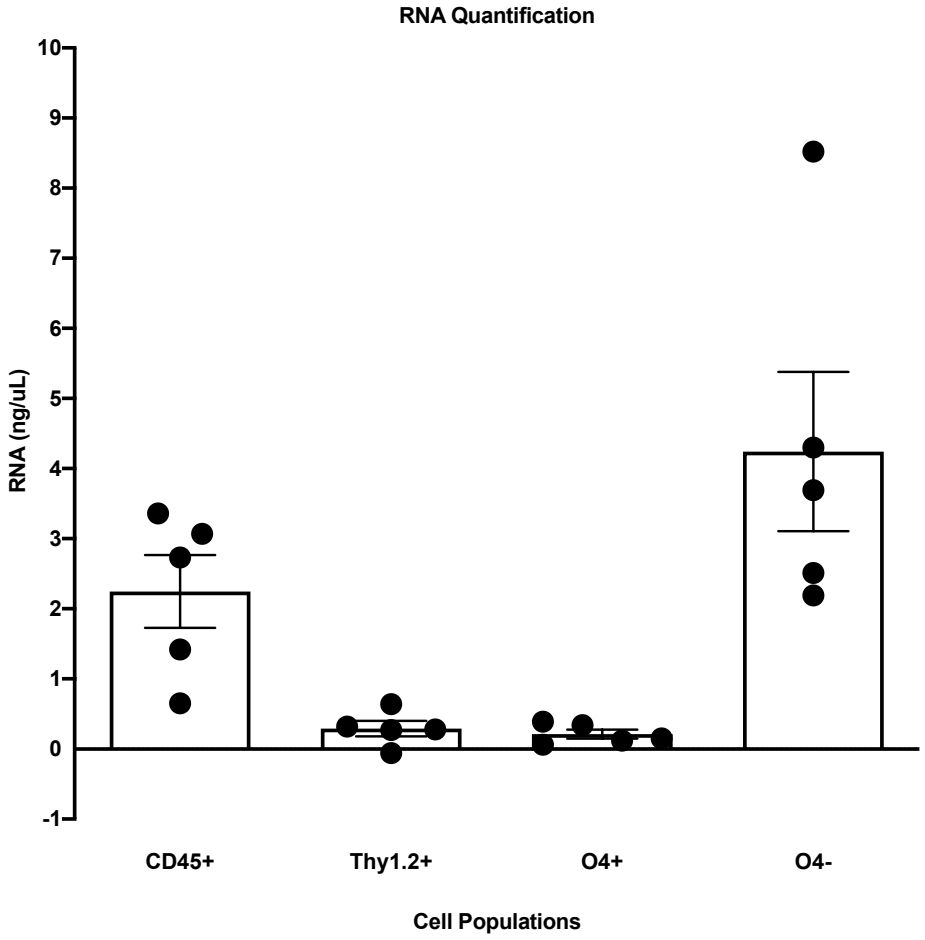

Figure 4. RNA quantification of different cell populations in Immunopanning Trial 2

III. Fluorescence-activated cell sorting (FACS) of different cell populations in subcutaneous white adipose tissue

At the ages of 11 and 54 weeks, eight C57BL/6JUM mice were euthanized, and their inguinal subcutaneous white adipose depot was digested to isolate the stromal vascular fraction (SVF), which was then sorted into various cell populations which were isolated through the cell-sorting mechanism known as FACS. When comparing the adipose tissue of 11 week old mice to a 54 week old mice, there was a presence of p75+ cells with no significant difference between the age groups, a sub-population of cells positive for both CD45 and O4 with a statistically significant difference in the CD45+O4+ populations between the two age groups, as well as CD45+p75+ and CD45+O4-High sub-populations (Fig. 5, 6, 7). Although there were eight possible populations with the combinations of the three markers used, only five populations were noted and gated (exclusion of CD45+O4+p75+, CD45+O4-p75-, and CD45-O4+p75+ populations). There was a statistical significance between mice 11 weeks of age and 54 weeks of age in the cell populations labeled CD45+O4+p75- and CD45-O4-p75-. The relationship in the CD45+O4+p75- population was a negative correlation with age, while the CD45-O4-p75- population suggested a relationship that correlated positively with age (Fig. 8A). Outliers were included in Figure 8B, but when removed for further comparative analysis, there was still a significant statistical difference in the CD45+O4+p75- population.

A

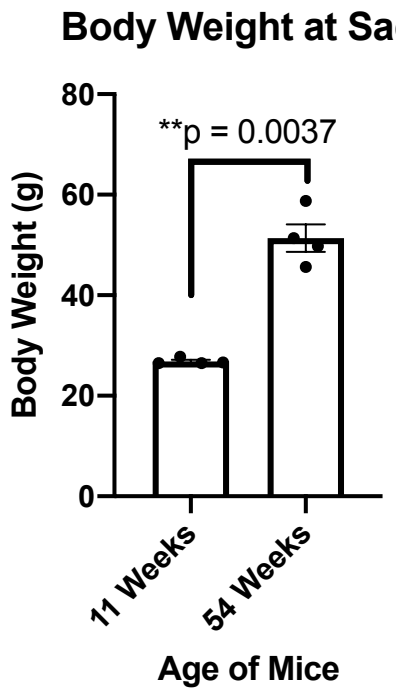

B

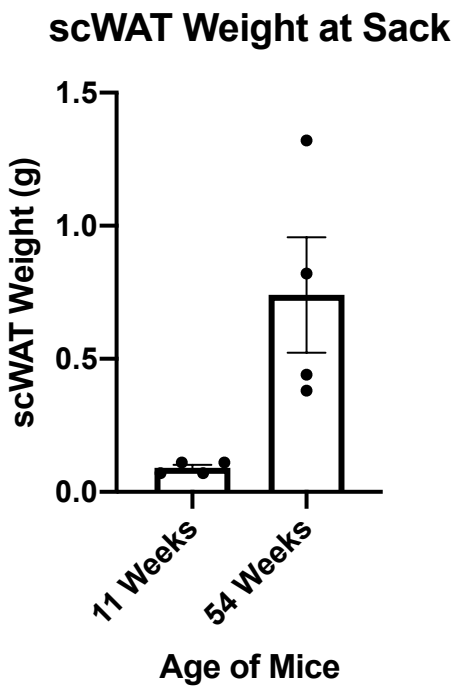

Figure 5. Weight differences between young and aged mice at tissue collection. (A) Body weight of mice 11 weeks old compared to body weight of mice 54 weeks old at time of tissue collection. **(B)** Subcutaneous white adipose tissue (scWAT) weight of mice 11 weeks old compared to scWAT of mice 54 weeks old at time of tissue collection.

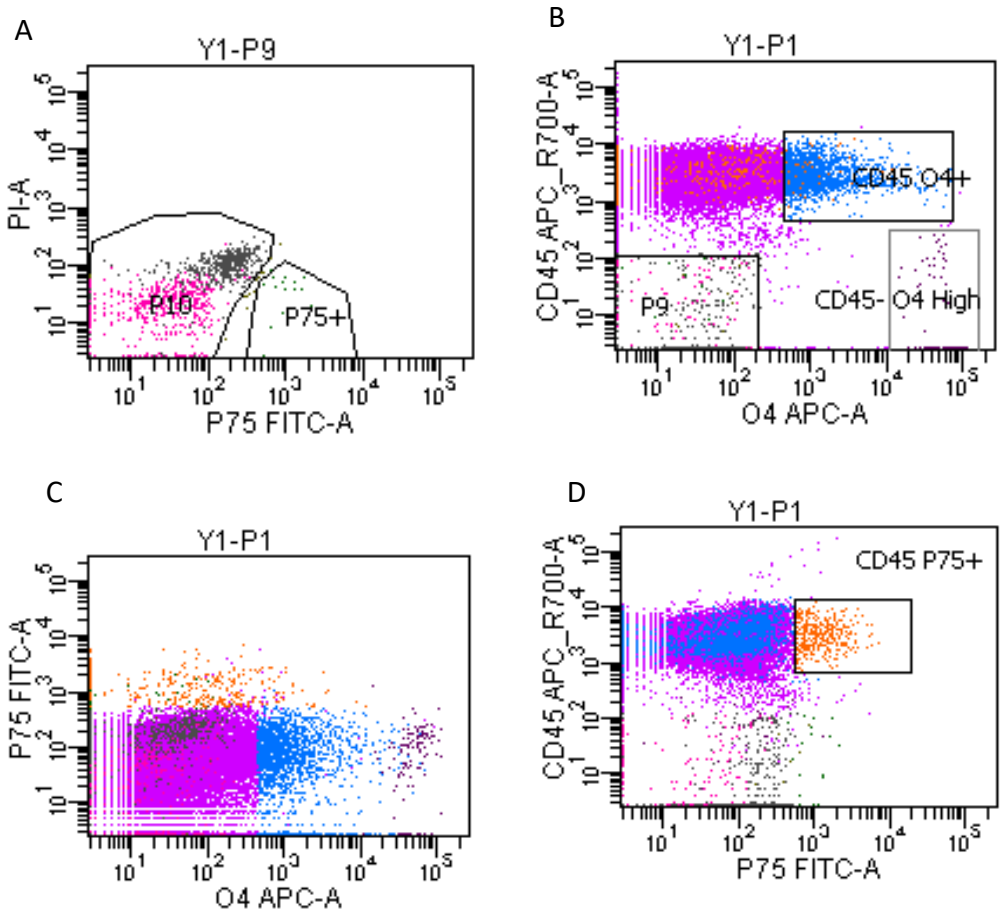

Figure 6. Density plots of the different cell populations represented in a young animal. (A) Density plot showing gate for p75+ cell population. **(B)** Density plot showing gate for CD45+O4+ cell population and CD45-O4-High cell population. **(C)** Density plot showing lack of existence of an O4+p75+ cell population. **(D)** Density plot showing gate for CD45+p75+ cell population.

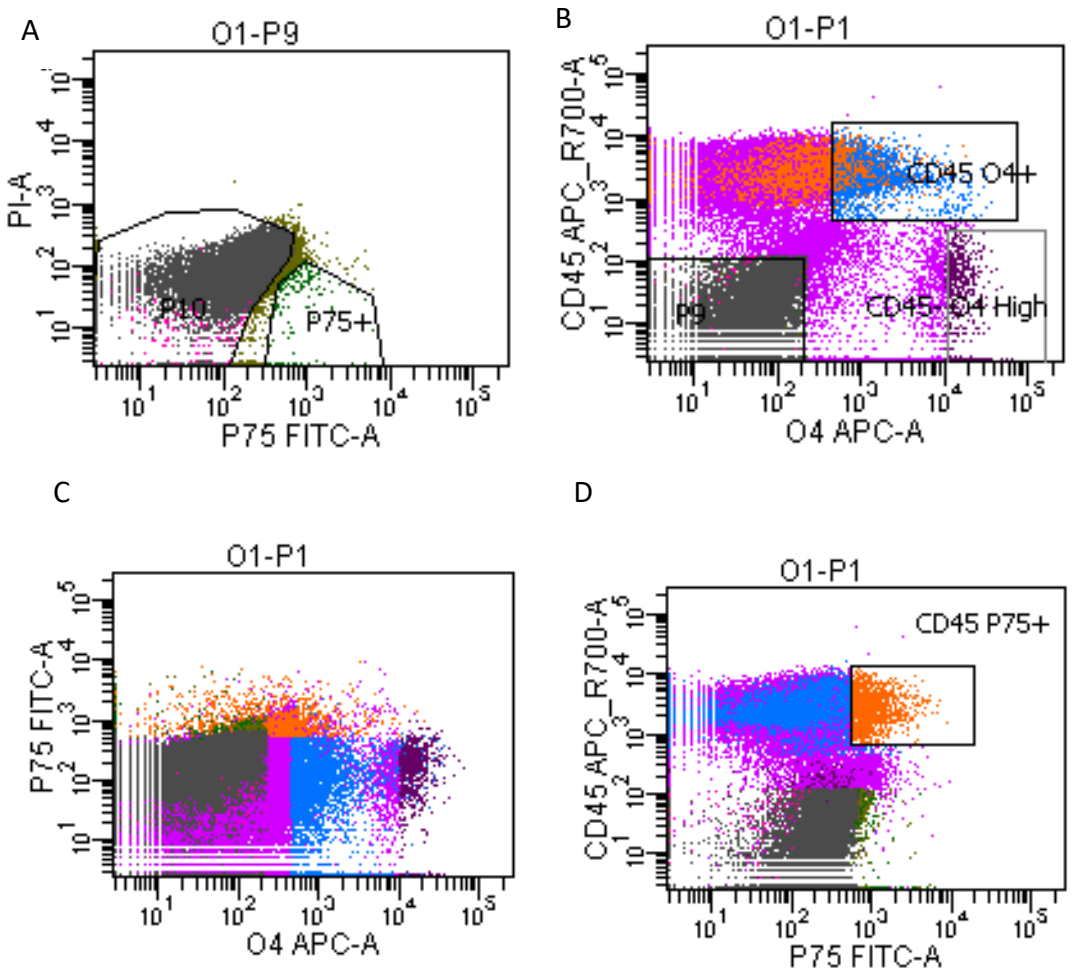

Figure 7. Density plots of the different cell populations represented in an old animal. **(A)** Density plot showing gate for p75+ cell population. **(B)** Density plot showing gate for CD45+O4+ cell population and CD45-O4-High cell population. **(C)** Density plot showing lack of existence of an O4+p75+ cell population. **(D)** Density plot showing gate for CD45+p75+ cell population.

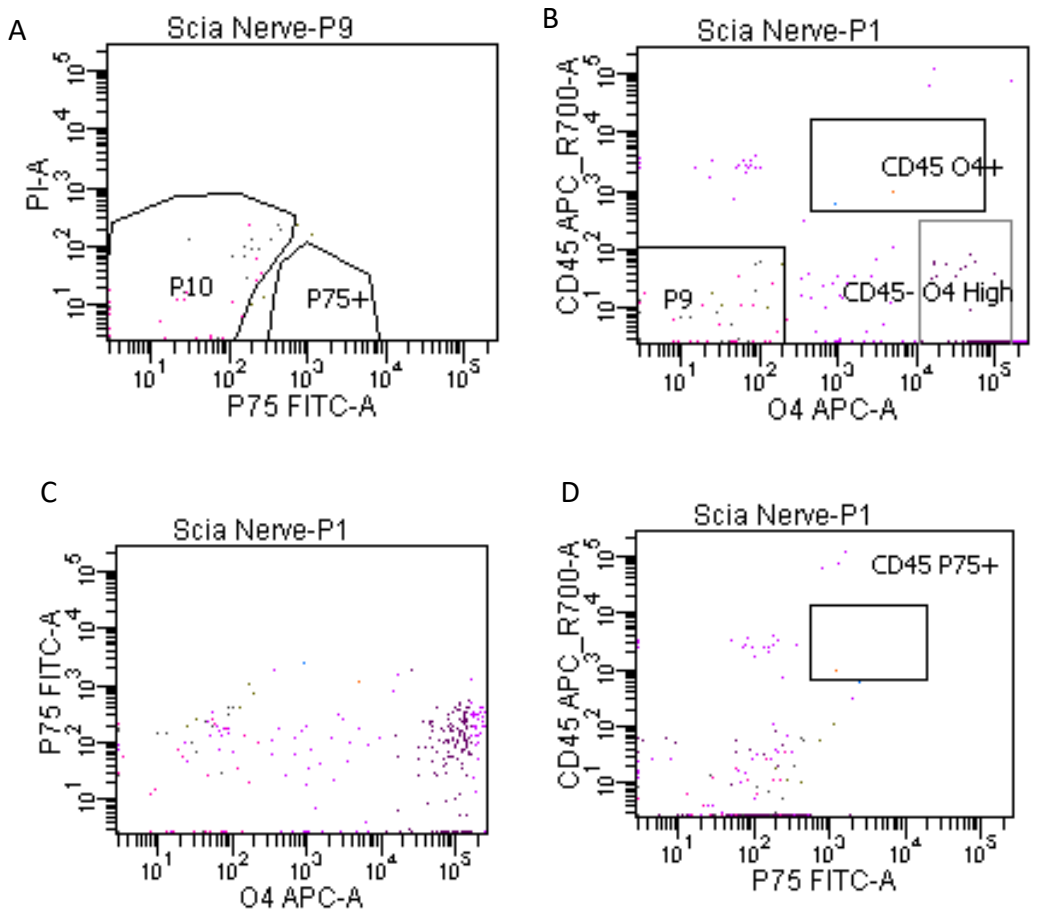

Figure 8. Density plots of the different cell populations represented in sciatic nerve. **(A)** Density plot showing gate for p75+ cell population. **(B)** Density plot showing gate for CD45+O4+ cell population and CD45-O4-High cell population. **(C)** Density plot showing lack of existence of an O4+p75+ cell population. **(D)** Density plot showing gate for CD45+p75+ cell population.

Cell populations expressing only O4, used commonly as a marker of mature oligodendroyctes in the CNS and Schwann cells in the PNS, conveyed no statistically significant difference between populations of mice aged 11 weeks and those aged 54 weeks (Fig. 9). Comparisons were done for both the total cell population and the percent

cell count. Similarly, total cell populations and percent cell counts expressing CD45+O4+p75- were measured and compared in mice ages 11 weeks and 54 weeks old (Fig. 10). There was a statistically significant decrease in the aged cohort of mice compared to the young cohort (Fig. 10B).

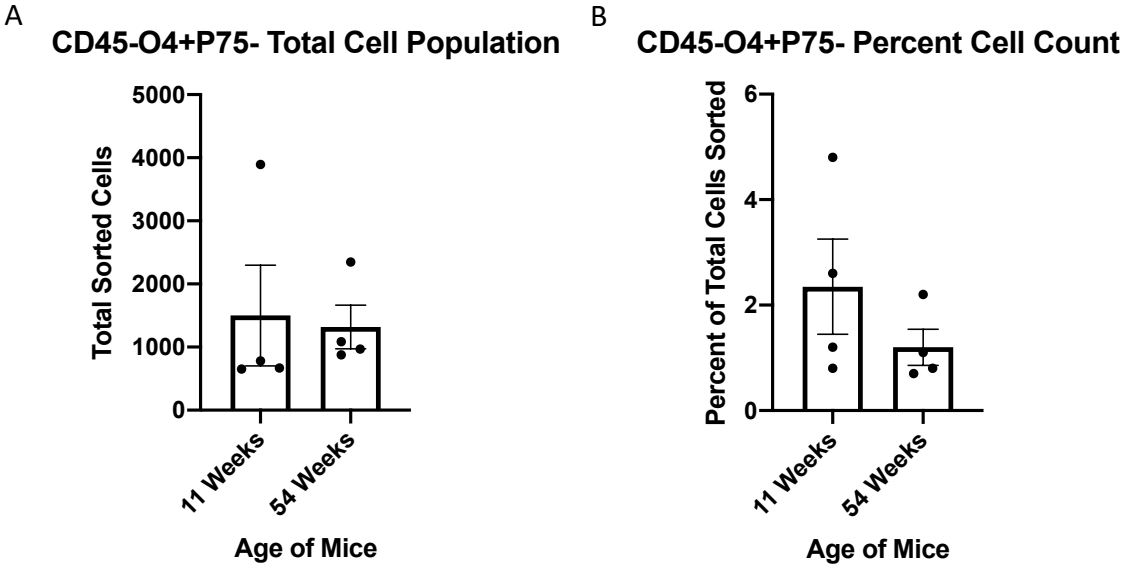

Figure 9. Population in scWAT expressing only myelin marker O4 in young mice compared to aged mice. (A) Total cell population of cells expressing CD45-O4+p75- in mice 11 weeks and 54 weeks old. **(B)** Percent cell count of cells expressing CD45-O4+p75- in mice 11 weeks and 54 weeks old.

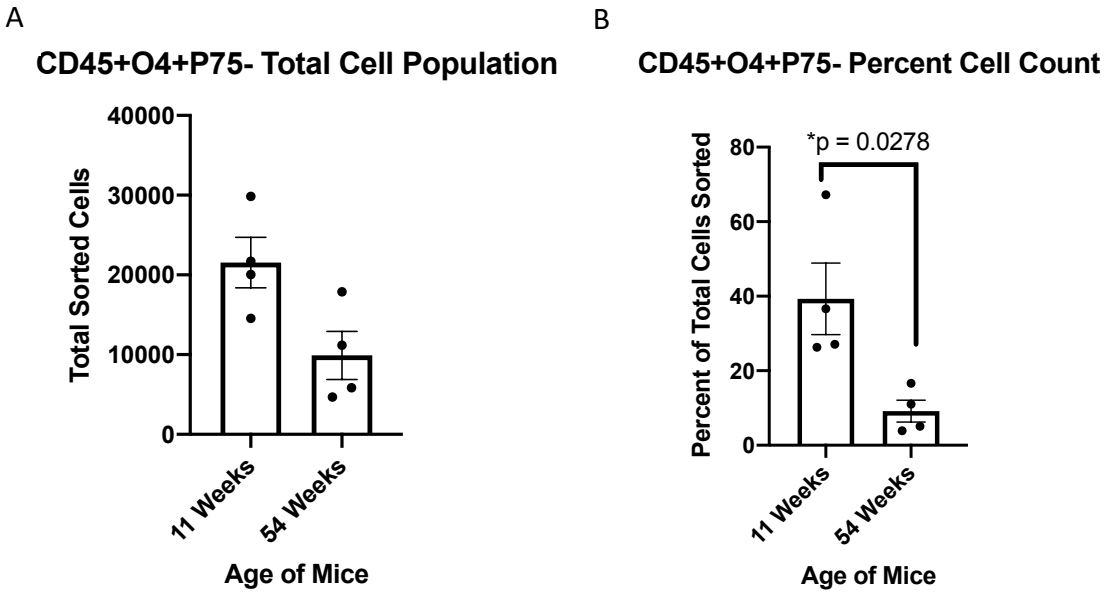

Figure 10. Population in scWAT expressing myelin marker O4 and common leukocyte marker CD45 in young mice compared to aged mice. (A) Total cell population of cells expressing CD45+O4+p75- in mice 11 weeks and 54 weeks old. **(B)** Percent cell count of cells expressing CD45+O4+p75- in mice 11 weeks and 54 weeks old.

As a categorical marker of Schwann cells throughout their developmental lineage, p75 showed expression in two different populations (Fig. 11). Comparisons were done for both the total cell population and the percent cell count of CD45+O4-p75+ (Fig. 11A, 11B). Similarly, total cell populations and percent cell counts expressing CD45-O4-p75+ were measured and compared in mice ages 11 weeks and 54 weeks old (Fig. 11C, 11D).

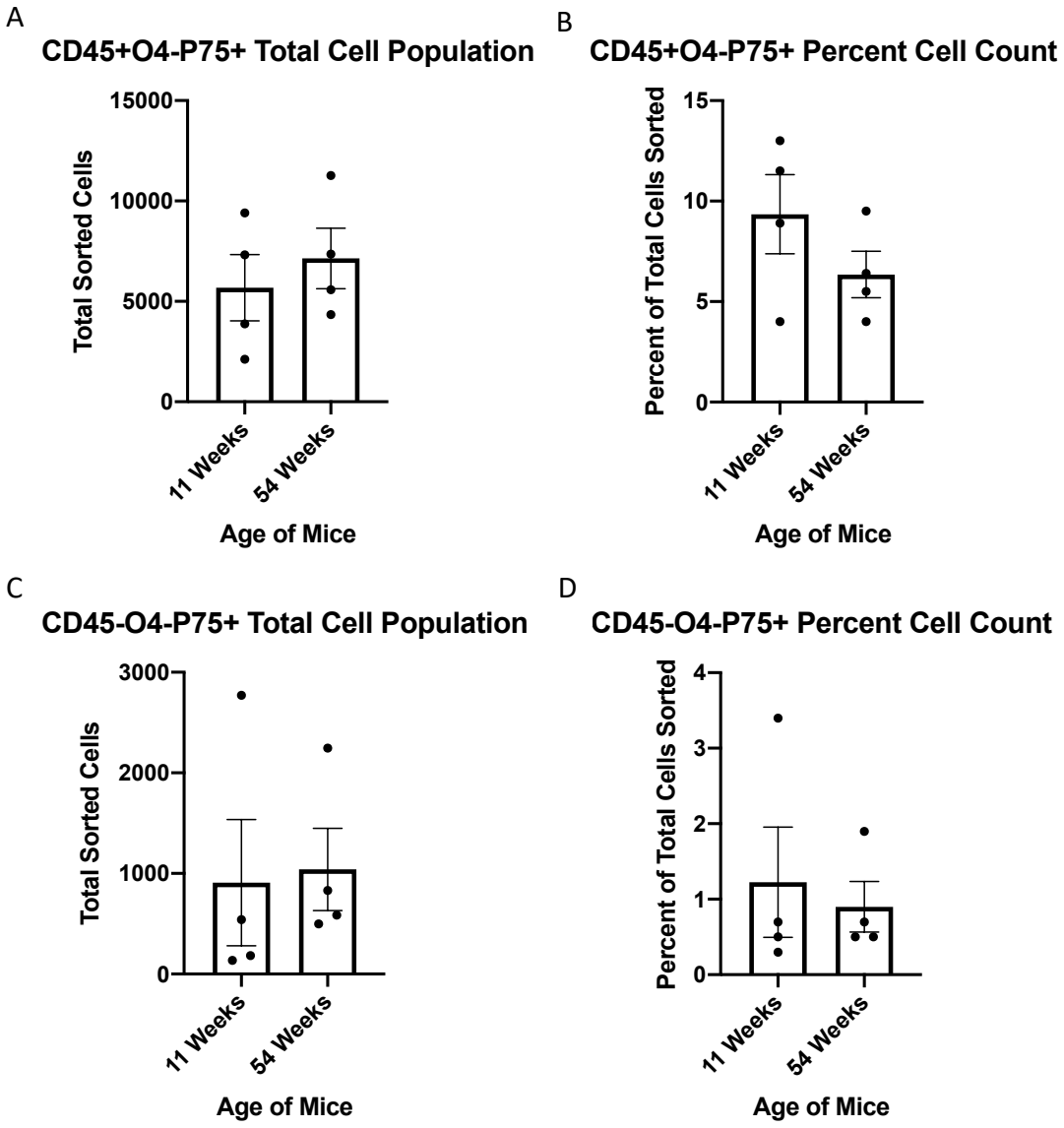

Figure 11. Populations of cells in scWAT expressing p75. (A) Total cell population of cells expressing CD45+O4-p75+ in mice 11 weeks and 54 weeks old. **(B)** Percent cell count of cells expressing CD45+O4-p75+ in mice 11 weeks and 54 weeks old. **(C)** Total cell population of cells expressing CD45-O4-p75+ in mice 11 weeks and 54 weeks old. **(D)** Percent cell count of cells expressing CD45-O4-p75+ in mice 11 weeks and 54 weeks old.

The five cell populations were plotted relative to body weight. The two populations that showed statistical significance were again, the CD45+O4+p75- population and CD45-O4-p75- population; the former showing a negative correlation with percentage of total cells to body weight and the latter showing a positive correlation with percentage of total cells to body weight.

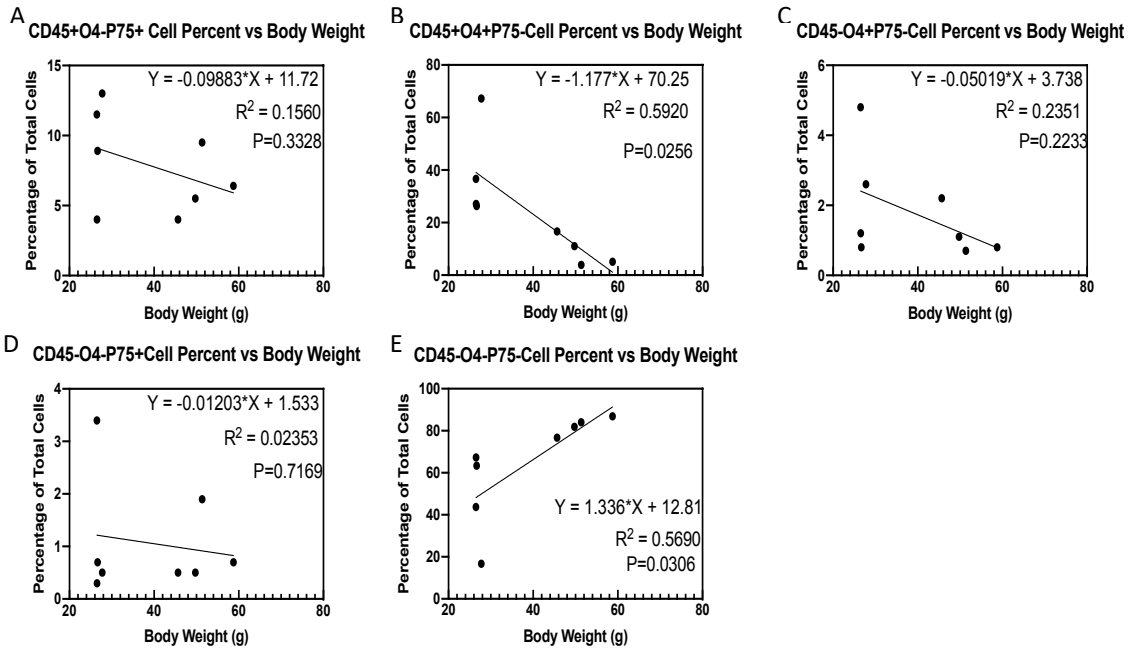

Figure 12. Correlation between population cell percentage and body weight.

(A) The correlation between the CD45+O4-p75+ population cell percentage and body weight. **(B)** The correlation between the CD45+O4+Pp5- population cell percentage and body weight. **(C)** The correlation between the CD45-O4+p75- population cell percentage and body weight. **(D)** The correlation between the CD45-O4-p75+ population cell percentage and body weight, and **(E)** The correlation between the CD45-O4-p75- population cell percentage and body weight.

The five cell populations were also plotted relative to adipose weight. The only population that showed statistical significance in these plots was the CD45+O4+p75- population. This population showed a negative correlation between percentage of total cells and adipose weight.

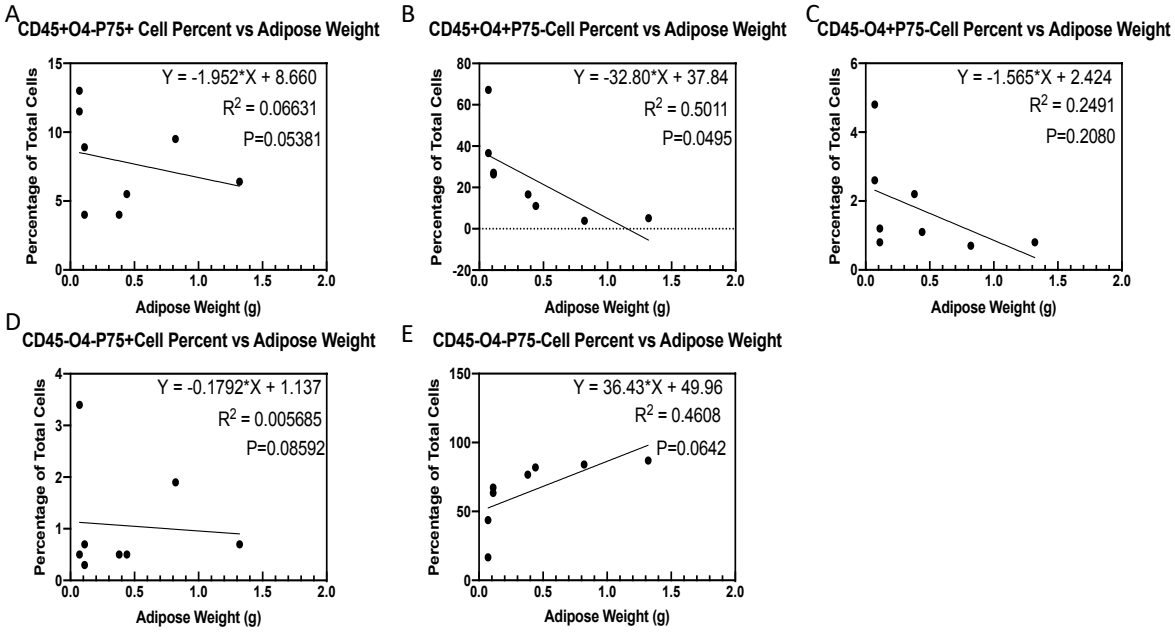

Figure 13. Correlation between population cell percentage and adipose weight.

(A) The correlation between the CD45+O4-p75+ population cell percentage and adipose weight. **(B)** The correlation between the CD45+O4+p75- population cell percentage and adipose weight. **(C)** The correlation between the CD45-O4+p75- population cell percentage and adipose weight. **(D)** The correlation between the CD45-O4-p75+ population cell percentage and adipose weight, and **(E)** The correlation between the CD45-O4-p75- population cell percentage and adipose weight.

DISCUSSION

While there is still an exorbitant amount of information that remains unanswered about the mechanisms and roles of Schwann cells, there is even less information about their roles in adipose tissue and therefore a lack of knowledge regarding implications of the presence (or lack thereof) of Schwann cells in neuropathy in the subcutaneous adipose depot. The phenotypic plasticity of Schwann cells constitutes their continuation as an enigma in the peripheral nervous system, although researchers are slowly chipping away at their various developmental stages, phenotypes, and associated roles and molecular markers[33]. White adipose tissue is characteristically known for its role in energy storage and for adipocytes being the major cellular constituent of the tissue. Only recently has the importance of subcutaneous WAT and its innervation been recognized for its role in peripheral neuropathy[17]. As this has been recent discussion, there hasn't been much focus – or any, really – on the existence of Schwann cells in adipose tissue and their role in nerve health in these depots.

Immunopanning

Such low levels of RNA extracted from all cell populations in immunopanning trials I and II are likely a result of there not being a large number of cells in each population present in adipose tissue taken from a singular animal. While the left and right depots were pooled, the depots from each individual animal were analyzed separately for integrity. The extremity to which the RNA levels were low requires RNA amplification before conversion to cDNA for analysis via quantitative polymerase chain reaction

(qPCR) can occur. Finding an RNA amplification kit that works for the samples taken and that is compatible with downstream Green SYBR chemistry for qPCR proved to be a bit of a hassle. qPCR is a necessary technique that allows the samples to be analyzed for gene expression of various genes. The major goal of this is two-fold; to ensure the cell population isolated on each dish were congruent with what was anticipated, and to see what characteristic markers of Schwann cells were expressed by the O4+ population, as that population was anticipated to be solely Schwann cells. While there is a presence of O4+ cells in both immunopanning trials I and II, it would be preemptive to claim solely from this data that this population is Schwann cells. Also, it is important to note that results from immunopanning trial II are more reliable for the reason that the collagenase used in immunopanning trial I didn't digest the tissue as well as we had hoped, so we switched to collagenase A in the second trial and had much better luck with the digestion of the adipose tissue.

FACS

The antibodies chosen for the FACS experiments were done so strategically. The marker p75 is notorious for its role in marking both Schwann cell precursors (SCPs) and non-myelinating Schwann cells, or Remak cells, as well as sometimes being used as a marker of Schwann cells in general [52–54]. As seen in Figure 11, there was a presence of a CD45+p75+ cell population as well as a solely p75+ cell population. Interestingly, there was cell population that we gated indicating an overlapping presence of both of the markers for O4 and p75. This is an intriguing note, as both have been used as markers for mature Schwann cells in literature, yet there appears to be no overlapping population in

the adipose tissues taken from the mice in this experiment. This could be indicative of a niche population solely expressing p75 or one expressing both p75 and the common leukocyte marker CD45. There was, however, a surprisingly low number of p75 cells. This information combined with the lack of p75+/O4+ overlap, may suggest the need to look at other antibody options, as some antibodies are tissue specific and therefore work better in some tissues than others. When comparing the two age populations (mice at 11 weeks versus mice at 54 weeks), there was no statistically significant difference. This indicates that age may not be an important factor in the number of SCPs or non-myelinating Schwann cells present in the inguinal subcutaneous white adipose tissue. Debatably, as age is historically a causative agent of peripheral neuropathy, these two Schwann cell phenotypes may not be critical to preventing peripheral neuropathy and maintaining nerve health in this manner.

There was also a sub-population of cells identified to be only O4+. Oligodendrocyte marker 4 (O4) was chosen as a marker for myelinating Schwann cells. Oligodendrocytes are the myelinating cell of the CNS and are quite similar to Schwann cells in that regard. Therefore, O4 was previously used in the Cold Spring Harbor protocol referenced for isolating and purifying Schwann cells, and is used throughout the literature for marking myelinating Schwann cells[49,55]. The presence of O4+ cells does further reiterate our findings from the immunopanning trials that there are myelinating cells in these tissues. While these cells appear to have a negative trend with age, there is no significant difference in total cell percentage between age groups. Comparatively to the CD45+O4+ sub-population, this sub-population of exclusively O4+ cells constitutes a miniscule percentage of the entire cell population.

The sub-population of cells sorted that commands the most attention is that of the CD45+O4+. Cluster of differentiation 45 (CD45) is a known common leukocyte marker. This is of interest, because leukocytes are responsible for the body's immune response through a widespread variety of mechanisms. Distinguishing cells with this marker is critical, as the role of Schwann cells in immune responses is still being researched intensely. Schwann cells are known for both their ability to recruit high levels of leukocytes, such as macrophages and neutrophils, post-injury, as well as their ability to change phenotypically to help in the axonal repair process[45,52,53]. During the sort, the CD45+O4+ quickly became the most intriguing subset of cells. These cells both expressed a marker well known for marking myelination, but also a very typical marker of immune cells. These results indicate that there is a phenotypic population of cells expressing proteins typically concurrent with myelination, that are also expressing the same proteins as many leukocytes. This is a very interesting finding, as it reiterates the potential role of Schwann cells (or Schwann-like cells) in immunity and repair. Additionally, this population was the only population (aside from that reading negative to all markers), that had a significant difference between age groups. Mice at the age of 11 weeks showed a significantly higher percentage of total cells that were CD45+O4+ when compared to mice at the age of 54 weeks. As mentioned before, aging is a common trigger for peripheral neuropathy, indicative of a correlation to declining nerve health. There are also many neuropathies that develop as a result of demyelination [45]. The significant decline in total cell percentage of cells that are CD45+O4+ is extremely intriguing, as this is a group of cells previously unidentified to our knowledge. To further

identify what these cells may be and their potential role in adipose and/or nerve health, we must use qPCR to confirm gene expression.

Another intriguing difference to note is that in the sub-population of cells that were negative for all markers, there was a statistical significance between age groups. In this scenario, however, the opposite difference from the CD45+O4+ sub-population was found, and the total percentage of cells that were negative for all markers *increased* significantly with age. A hypothesis to consider is that as individuals age and cells become senescent, they stop exhibiting the proteins responsible for immune responses and myelination, and therefore fall into a category of no expression.

In Figures 12 and 13, the total cell percentages of each sub-population were graphed relative to body weight (Fig. 12) and adipose weight (Fig. 13). Figure 12B shows a statistically significant negative correlation between body weight (g) and total percentage of CD45+O4+ cells. This finding carries over to Figure 13B, showing a statistically significant negative correlation between adipose weight (g) and total percentage of CD45+O4+ cells. Together, these results indicate that as body weight and adipose weight increase, the number of CD45+O4+ cells decrease. This is relevant when considering implications of the obesity epidemic. Literature shows that increased obesity leads to many co-morbidities, including those previously listed in this thesis. If this sub-population of cells (CD45+O4+) is critical for playing a role in maintaining nerve health, this data would suggest that as individuals become more obese, they are more likely to have a low percentage of these cells, and therefore are likely to have decreased maintenance of nerve health in adipose tissue. Furthermore, obesity is defined by a larger

fat mass, so the increased amount of fat would be pertinent to the fact that these cells have been labeled in adipose tissue.

FUTURE DIRECTIONS

Now that the immunopanning protocol has had most of its kinks worked out, further experiments can be conducted using the developed protocol. Upon arrival of the RNA amplification kit in the Townsend Lab, the RNA from both immunopanning trials and FACS experiments can be amplified and converted into cDNA, at which point the gene expression of the differing cell populations can be confirmed using primers we have already designed for qPCR. Once the cell types in these populations are confirmed, further conclusions can be drawn – from the immunopanning trials particularly.

Additionally, other antibodies can be used in the immunopanning protocol to isolate different cell populations and speculate for previously unidentified ones. For instance, there may be populations of cells exhibiting markers characteristic of other glia or immune cell types that have yet to identified in adipose tissue. Emerging glial cells and their respective roles are becoming apparent in areas such as the enteric nervous system, so speculating the possibility of similar cell types residing in the adipose tissue and playing an imperative role in nerve health is not unrealistic.

Furthermore, FACS can continue to be used as way to sort live cell populations. Further studies should include valid young vs. aged cohort of females and one of males to compare potential sex differences. Other interventions of interest that may show important effects on adipose tissue are that of a high-fat diet and a cold versus room temperature, respectively. As the FACS experiment in this thesis indicates a correlation between adipose weight and sub-population of cells, it would be of interest to induce obesity through a high-fat diet and compare sub-populations (such as that of CD45+O4+)

in these mice relative to healthy mice. We have also seen that cold interventions exhibit an increase in GAP43, a marker that indicates axonal cone outgrowth[17]. It would be interesting to see how cell populations change over time based on cold exposure. If axonal cone outgrowth increases in the cold and if cell sub-populations, such as CD45+O4+, prove critical for nerve health or repair, it may be hypothesized that sub-populations such as this will also increase due to cold exposure.

REFERENCES

1. Apovian, C.M. (2016). Obesity: Definition, Comorbidities, Causes, and Burden. THE AMERICAN JOURNAL OF MANAGED CARE *22*, 10.

2. Obesity and overweight Available at: https://www.who.int/news-room/fact-sheets/detail/obesity-and-overweight [Accessed February 5, 2020].

3. Hunger & Obesity Food Research & Action Center. Available at: https://frac.org/hunger-obesity [Accessed February 5, 2020].

4. CDC (2020). New Adult Obesity Maps. Centers for Disease Control and Prevention. Available at: https://www.cdc.gov/obesity/data/prevalence-maps.html [Accessed February 5, 2020].

5. Lynes, M.D., and Tseng, Y.-H. (2018). Deciphering adipose tissue heterogeneity. Annals of the New York Academy of Sciences *1411*, 5–20.

6. Jura, M., and Kozak, Leslie.P. (2016). Obesity and related consequences to ageing. Age (Dordr) *38*. Available at: https://www.ncbi.nlm.nih.gov/pmc/articles/PMC5005878/ [Accessed April 22, 2020].

7. Diagnosis and Classification of Diabetes Mellitus - ProQuest Available at: https://search.proquest.com/openview/2b3d46bde605248741710523e4607916/1?cbl=47715&pq-origsite=gscholar [Accessed February 5, 2020].

8. Blood Sugar and Insulin at Work | ADA Available at: https://www.diabetes.org/diabetes-risk/prevention/high-blood-sugar [Accessed February 5, 2020].

9. Liu, X., Xu, Y., An, M., and Zeng, Q. (2019). The risk factors for diabetic peripheral neuropathy: A meta-analysis. PLoS One *14*. Available at: https://www.ncbi.nlm.nih.gov/pmc/articles/PMC6382168/ [Accessed January 25, 2020].

10. Jolivalt, C.G., Frizzi, K.E., Guernsey, L., Marquez, A., Ochoa, J., Rodriguez, M., and Calcutt, N.A. (2016). PHENOTYPING PERIPHERAL NEUROPATHY IN MOUSE MODELS OF DIABETES. Curr Protoc Mouse Biol *6*, 223–255.

11. Stino, A.M., and Smith, A.G. (2017). Peripheral neuropathy in prediabetes and the metabolic syndrome. J Diabetes Investig *8*, 646–655.

12. Hicks, C.W., and Selvin, E. (2019). Epidemiology of Peripheral Neuropathy and Lower Extremity Disease in Diabetes. Curr Diab Rep *19*, 86.

13. Yagihashi, S., Mizukami, H., and Sugimoto, K. (2011). Mechanism of diabetic neuropathy: Where are we now and where to go? J Diabetes Investig *2*, 18–32.

14. Blaszkiewicz, M., Willows, J.W., Johnson, C.P., and Townsend, K.L. (2019). The Importance of Peripheral Nerves in Adipose Tissue for the Regulation of Energy Balance. Biology (Basel) *8*. Available at: https://www.ncbi.nlm.nih.gov/pmc/articles/PMC6466238/ [Accessed January 25, 2020].

15. Townsend, K., and Tseng, Y.-H. (2012). Brown adipose tissue. Adipocyte *1*, 13–24.

16. Foster, M.T., and Bartness, T.J. (2006). Sympathetic but not sensory denervation stimulates white adipocyte proliferation. American Journal of Physiology-Regulatory, Integrative and Comparative Physiology *291*, R1630–R1637.

17. Blaszkiewicz, M., Willows, J.W., Dubois, A.L., Waible, S., DiBello, K., Lyons, L.L., Johnson, C.P., Paradie, E., Banks, N., Motyl, K., *et al.* (2019). Neuropathy and neural plasticity in the subcutaneous white adipose depot. PLoS One *14*. Available at: https://www.ncbi.nlm.nih.gov/pmc/articles/PMC6738614/ [Accessed January 25, 2020].

18. Shi, H., Song, C.K., Giordano, A., Cinti, S., and Bartness, T.J. (2005). Sensory or sympathetic white adipose tissue denervation differentially affects depot growth and cellularity. American Journal of Physiology-Regulatory, Integrative and Comparative Physiology *288*, R1028–R1037.

19. Blaszkiewicz, M., and Townsend, K.L. (2016). Adipose Tissue and Energy Expenditure: Central and Peripheral Neural Activation Pathways. Curr Obes Rep *5*, 241–250.

20. Zeng, W., Pirzgalska, R.M., Pereira, M.M.A., Kubasova, N., Barateiro, A., Seixas, E., Lu, Y.-H., Kozlova, A., Voss, H., Martins, G.G., *et al.* (2015). Sympathetic Neuro-adipose Connections Mediate Leptin-Driven Lipolysis. Cell *163*, 84–94.

21. Chang, J.C., Durinck, S., Chen, M.Z., Martinez-Martin, N., Zhang, J.A., Lehoux, I., Li, H., Lin, M., Wu, J., Bainbridge, T.W., *et al.* (2019). Adaptive adipose tissue stromal plasticity in response to cold stress and antibody-based metabolic therapy. Sci Rep *9*. Available at: https://www.ncbi.nlm.nih.gov/pmc/articles/PMC6586812/ [Accessed February 7, 2020].

22. Which U.S. States Have the Oldest Populations? – Population Reference Bureau Available at: https://www.prb.org/which-us-states-are-the-oldest/ [Accessed April 23, 2020].

23. Popescu, S., Timar, B., Baderca, F., Simu, M., Diaconu, L., Velea, I., and Timar, R. (2016). Age as an independent factor for the development of neuropathy in diabetic patients. Clin Interv Aging *11*, 313–318.

24. Purves, D., Augustine, G.J., Fitzpatrick, D., Katz, L.C., LaMantia, A.-S., McNamara, J.O., and Williams, S.M. (2001). Neuroglial Cells. Neuroscience. 2nd edition. Available at: https://www.ncbi.nlm.nih.gov/books/NBK10869/ [Accessed February 9, 2020].

25. Siracusa, R., Fusco, R., and Cuzzocrea, S. (2019). Astrocytes: Role and Functions in Brain Pathologies. Front Pharmacol *10*. Available at: https://www.ncbi.nlm.nih.gov/pmc/articles/PMC6777416/ [Accessed February 9, 2020].

26. Galloway, D.A., Phillips, A.E.M., Owen, D.R.J., and Moore, C.S. (2019). Phagocytosis in the Brain: Homeostasis and Disease. Front Immunol *10*. Available at: https://www.ncbi.nlm.nih.gov/pmc/articles/PMC6477030/ [Accessed February 9, 2020].

27. Augusto-Oliveira, M., Arrifano, G.P., Lopes-Araújo, A., Santos-Sacramento, L., Takeda, P.Y., Anthony, D.C., Malva, J.O., and Crespo-Lopez, M.E. (2019). What Do Microglia Really Do in Healthy Adult Brain? Cells *8*. Available at: https://www.ncbi.nlm.nih.gov/pmc/articles/PMC6829860/ [Accessed February 9, 2020].

28. Kuhn, S., Gritti, L., Crooks, D., and Dombrowski, Y. (2019). Oligodendrocytes in Development, Myelin Generation and Beyond. Cells *8*.

29. Enes, J., Haburčák, M., Sona, S., Gerard, N., Mitchell, A.C., Fu, W., and Birren, S.J. (2020). Satellite glial cells modulate cholinergic transmission between sympathetic neurons. PLoS ONE *15*, e0218643.

30. Jessen, K.R., and Mirsky, R. (2019). Schwann Cell Precursors; Multipotent Glial Cells in Embryonic Nerves. Front Mol Neurosci *12*, 69.

31. Dyachuk, V., Furlan, A., Shahidi, M.K., Giovenco, M., Kaukua, N., Konstantinidou, C., Pachnis, V., Memic, F., Marklund, U., Müller, T., *et al.* (2014). Parasympathetic neurons originate from nerve-associated peripheral glial progenitors. Science *345*, 82–87.

32. Espinosa-Medina, I., Outin, E., Picard, C.A., Chettouh, Z., Dymecki, S., Consalez, G.G., Coppola, E., and Brunet, J.-F. (2014). Parasympathetic ganglia derive from Schwann cell precursors. Science *345*, 87–90.

33. Jessen, K.R., Mirsky, R., and Lloyd, A.C. (2015). Schwann Cells: Development and Role in Nerve Repair. Cold Spring Harb Perspect Biol *7*. Available at: https://www.ncbi.nlm.nih.gov/pmc/articles/PMC4484967/ [Accessed January 23, 2020].

34. Fallon, M., and Tadi, P. (2019). Histology, Schwann Cells (StatPearls Publishing) Available at: https://www.ncbi.nlm.nih.gov/books/NBK544316/ [Accessed March 31, 2020].

35. Court, F.A., Wrabetz, L., and Feltri, M.L. (2006). Basal lamina: Schwann cells wrap to the rhythm of space-time. Current Opinion in Neurobiology *16*, 501–507.

36. Simons, M., Snaidero, N., and Aggarwal, S. (2012). Cell polarity in myelinating glia: From membrane flow to diffusion barriers. Biochimica et Biophysica Acta (BBA) - Molecular and Cell Biology of Lipids *1821*, 1146–1153.

37. Laura, F.M., Yannick, P., and Carlo, P.S. (2016). How Schwann Cells Sort Axons: New Concepts. Neuroscientist *22*, 252–265.

38. Simons, M., Krämer, E.-M., Thiele, C., Stoffel, W., and Trotter, J. (2000). Assembly of Myelin by Association of Proteolipid Protein with Cholesterol- and Galactosylceramide-Rich Membrane Domains. J Cell Biol *151*, 143–154.

39. Ino, D., Sagara, H., Suzuki, J., Kanemaru, K., Okubo, Y., and Iino, M. (2015). Neuronal Regulation of Schwann Cell Mitochondrial Ca2+ Signaling during Myelination. Cell Reports *12*, 1951–1959.

40. Medeiros, R.C.A., Girardi, K. do C. de V., Cardoso, F.K.L., Mietto, B. de S., Pinto, T.G. de T., Gomez, L.S., Rodrigues, L.S., Gandini, M., Amaral, J.J., Antunes, S.L.G., *et al.* (2016). Subversion of Schwann Cell Glucose Metabolism by Mycobacterium leprae. J Biol Chem *291*, 21375–21387.

41. Ino, D., and Iino, M. (2017). Schwann cell mitochondria as key regulators in the development and maintenance of peripheral nerve axons. Cell. Mol. Life Sci. *74*, 827–835.

42. Jessen, K.R., and Mirsky, R. (2008). Negative regulation of myelination: Relevance for development, injury, and demyelinating disease. Glia *56*, 1552–1565.

43. Arthur-Farraj, P.J., Latouche, M., Wilton, D.K., Quintes, S., Chabrol, E., Banerjee, A., Woodhoo, A., Jenkins, B., Rahman, M., Turmaine, M., *et al.* (2012). c-Jun Reprograms Schwann Cells of Injured Nerves to Generate a Repair Cell Essential for Regeneration. Neuron *75*, 633–647.

44. Jessen, K.R., and Arthur-Farraj, P. (2019). Repair Schwann cell update: Adaptive reprogramming, EMT, and stemness in regenerating nerves. Glia *67*, 421–437.

45. Park, H.T., Kim, J.K., and Tricaud, N. (2019). The conceptual introduction of the "demyelinating Schwann cell" in peripheral demyelinating neuropathies. Glia *67*, 571–581.

46. Preparation of separate astroglial and oligodendroglial cell cultures from rat cerebral tissue (1980). J Cell Biol *85*, 890–902.

47. Barres, B.A., Silverstein, B.E., Corey, D.P., and Chun, L.L.Y. (1988). Immunological, morphological, and electrophysiological variation among retinal ganglion cells purified by panning. Neuron *1*, 791–803.

48. Assouline, JoséG., Bosch, E.P., and Lim, R. (1983). Purification of rat Schwann cells from cultures of peripheral nerve: an immunoselective method using surfaces coated with anti-immunoglobulin antibodies. Brain Research *277*, 389–392.

49. Lutz, A.B. (2014). Purification of Schwann Cells from the Neonatal and Injured Adult Mouse Peripheral Nerve. Cold Spring Harb Protoc *2014*, pdb.prot074989.

50. Fluorescence activated cell sorting of live cells | Abcam Available at: https://www.abcam.com/protocols/fluorescence-activated-cell-sorting-of-live-cells [Accessed April 11, 2020].

51. Liao, X., Makris, M., and Luo, X.M. (2016). Fluorescence-activated Cell Sorting for Purification of Plasmacytoid Dendritic Cells from the Mouse Bone Marrow. J Vis Exp. Available at: https://www.ncbi.nlm.nih.gov/pmc/articles/PMC5226086/ [Accessed April 11, 2020].

52. Lindborg, J.A., Mack, M., and Zigmond, R.E. (2017). Neutrophils Are Critical for Myelin Removal in a Peripheral Nerve Injury Model of Wallerian Degeneration. J Neurosci *37*, 10258–10277.

53. Stratton, J.A., Holmes, A., Rosin, N.L., Sinha, S., Vohra, M., Burma, N.E., Trang, T., Midha, R., and Biernaskie, J. (2018). Macrophages Regulate Schwann Cell Maturation after Nerve Injury. Cell Reports *24*, 2561-2572.e6.

54. Jessen, K.R., and Mirsky, R. (2019). The Success and Failure of the Schwann Cell Response to Nerve Injury. Front Cell Neurosci *13*. Available at: https://www.ncbi.nlm.nih.gov/pmc/articles/PMC6378273/ [Accessed April 11, 2020].

55. Shen, M., Tang, W., Cao, Z., Cao, X., and Ding, F. (2017). Isolation of rat Schwann cells based on cell sorting. Mol Med Rep *16*, 1747–1752.

APPENDICES

APPENDIX A

IACUC Letter of Approval

Office of Research Compliance
Institutional Animal Care and Use Committee

1865 THE UNIVERSITY OF MAINE

311 Alumni Hall
Orono, Maine 04469-5717
Tel: 207-581-2657
www.umaine.edu

December 17, 2019

To Whom It May Concern:

The Institutional Animal Care and Use Committee (IACUC) at the University of Maine has approved the following protocols:

Protocol #: A2019-01-03
Title: RESEARCH Innervation, Nerve Remodeling & Neurovascular Interactions in Adipose Tissue
Principal Investigator: Kristy Townsend (Magda Blaszkiewicz is listed as personnel on the protocol)
Date of Approval: 4/23/2019
Date of Expiration: 4/22/2022

Protocol #: A2017-09-04
Title: Adipose tissue neuropathy and neurotrophic factors project
Principal Investigator: Kristy Townsend (Magda Blaszkiewicz is listed as personnel on the protocol)
Date of Approval: 11/20/2017
Date of Expiration: 11/19/2020

Please contact Paula Portalatin, Research Compliance Officer III, 207-581-2657 or paula.portalatin@maine.edu with any questions.

Best regards,

Paula Portalatin
Research Compliance Officer III

APPENDIX B

List of Designed Primers for qPCR

PTPRC

Forward: ATGGTCCTCTGAATAAAGCCCA

Reverse: TCAGCACTATTGGTAGGCTCC

Thy1.2

Forward: CTGCCATCACTGAAGAAGCC

Reverse: TTCTGCCACCCTCACTACAG

Cldn11

Forward: ATGGTAGCCACTTGCCTTCAG

Reverse: AGTTCGTCCATTTTTCGGCAG

EGR2/Krox20

Forward: GTGGATGTGTTGTGGTGGTC

Reverse: TGGGATTTTGTCTACGGCCT

S100b

Forward: GCCCTCATTGATGTCTTCCACC

Reverse: GAACTCATGGCAGGCCGTGGTC

MPZ

Forward: GTCAAGTCCCCCAGTAGAA

Reverse: AGGAGCAAGAGGAAAGCAC

MBP

Forward: CAAGATGAAAACCCAGTAGTCCATT

Reverse: GAGGTGGTGTTCGAGGTGTCA

P75

Forward: GGTGATGGCAACCTCTACAGT

Reverse: CCTCGTGGGTAAAGGAGTCTA

GFAP

Forward: CGGAGACGCATCACCTCTG

Reverse: AGGGAGTGGAGGAGTCATTCG

AUTHOR'S BIOGRAPHY

Emma Paradie was born in Manchester, NH in 1998, but spent her entire childhood growing up in Auburn, ME, where she graduated from Edward Little High School in 2016. Emma is a Biology major with minors in neuroscience and psychology, and a concentration in pre-medical studies. While at the University of Maine, she has been able to be a part of some amazing communities. She has been a member of Operation H.E.A.R.T.S., for which she has been treasurer for the past two years; she has been a member of Partners for World Health, through which she was able to travel to Uganda on an incredible medical mission; she was able to found the undergraduate group of Women in STEMM (science, technology, engineering, math, and medicine) with two of her peers at UMaine; she has worked as a Maine Learning Assistant (MLA) for multiple classes and as a TA for an Honors Cultures and Contexts class, and has worked in the Townsend Lab for two and a half years. After graduation, she will be continuing research as a research assistant at The Ohio State for a year and then hopes to attend medical school and become a physician. One of her biggest dreams as a physician is to be able to volunteer a fair amount of time and medical assistance to developing nations around the globe.